Characterization of Advanced Magnetic Materials for Developing High-Power-Density High-Efficiency Electric Motors for Driving Electric Vehicles

Youguang Guo, Gang Lei
School of Electrical and Data Engineering
University of Technology Sydney
Sydney, Australia

Jianguo Zhu
School of Electrical and Computer Engineering
The University of Sydney
Sydney, Australia

***Abstract*—Advancing the performance and sustainability of electric vehicles (EVs) hinges on the development of high-power-density, high-efficiency electric motors and drives. This paper investigates the characterization of magnetic properties of advanced magnetic materials for enhancing the performance of these motors. It is crucial to comprehensively understand and model these material properties considering the specific operational conditions of these devices. For instance, the magnetic fields in rotating electrical machines exhibit rotational behavior either in a two-dimensional (2D) plane or across a three-dimensional (3D) space. Despite this, when designing and analyzing electrical machines, the material properties are often assessed under one-dimensional (1D) sinusoidal magnetization. Notably, research has unveiled stark differences between the 2D/3D rotational magnetic properties and their corresponding 1D counterparts. This paper endeavors to showcase the 2D/3D characterization of several electromagnetic materials such as soft magnetic composite, nanocrystalline, and amorphous ferromagnetic materials. Furthermore, it aims to explore their applications in advancing high-performance electric motors for EVs. Understanding these nuanced material behaviors across different dimensions of magnetization is vital for optimizing the design and efficiency of electric motors.**

Keywords—electric motor; electric vehicle; power density; efficiency; magnetic material; magnetic property characterization

I. INTRODUCTION

The electric vehicle (EV) industry is experiencing rapid growth as it seeks to address global environmental challenges and reduce dependence on fossil fuels. Central to this evolution is the development of efficient and powerful electric motor drives, which are pivotal in enhancing the performance, range, and overall viability of EVs [1,2]. The advancement of novel and sophisticated electromagnetic materials has been one key factor for creating these high-performance electric motors of high-efficiency, high-power-density, and highly reliability [3-8]. To fully harness the potential of these materials, a profound comprehension of the underlying physical mechanisms and suitable mathematical models is crucial for the advanced design and analysis of electromagnetic devices. Property models stand as a critical factor in the design of high-performance electric motors and the effective control of electric drive systems.

In the realm of electrical machine design and analysis, the widely used one-dimensional (1D) sinusoidal magnetic properties play a crucial role. Typically, these data are the primary information available, often provided by material suppliers or acquired through straightforward standard testing procedures in laboratories, e.g. Epstein frames [9,10]. The tester consists of two coils uniformly wound around the material specimen. In this setup, the first coil receives a current, enabling the determination of the magnetic field strength (H) within the material through the application of Ampere's Law. Meanwhile, the second coil remains open circuit, allowing for the measurement of its terminal voltage. By employing Faraday's Law, the magnetic flux density (B) within the sample is derived. Consequently, this process provides crucial information, specifically the B-H loops or curves, which depict the relationship between magnetic flux density and field strength. Furthermore, power loss curves associated with magnetic flux density and frequency are derived using Poynting's theorem based on the data. It is important to highlight that these measurements are conducted under conditions of so-called 1D magnetization, where the B and H directions are constrained to the same direction.

However, in a rotating electrical machine, the magnetic field operates in a fundamentally different manner, existing in a two-dimensional (2D) plane or a three-dimensional (3D) space. In this context, the orientations of B and H vectors typically differ. It has been observed that magnetic properties under 2D/3D rotational magnetization significantly deviate from those obtained via the standard 1D measurements using Epstein frames or ring samples [11-16]. Consequently, investigating the 2D/3D vectorial magnetic properties of magnetic materials holds substantial theoretical and practical significance.

This pursuit is particularly crucial in today's landscape as electric motors increasingly operate at higher speeds and frequencies to achieve high power density. Consequently, the core loss in these motors may constitute a significant portion of overall power loss, potentially exceeding even the losses incurred through copper conductors [17-19]. Understanding the 2D/3D vectorial magnetic properties becomes paramount in mitigating these core losses and optimizing the performance of high-speed electric motors [20].

This paper endeavors to provide a comprehensive overview of the characterization of advanced electromagnetic materials subjected to 2D/3D rotational magnetization. The primary goal is to facilitate the development of electric motors with enhanced features such as low specific power loss, high power density, and superior reliability, specifically targeted for application in electrified transportation. Section II introduces the testing systems employed to assess the rotational magnetic properties. Section III delves into the property measurement outcomes of some innovative electromagnetic materials. Section IV presents the magnetic property modeling considering the effects of 2D/3D rotational magnetization and its application in the design of 3D flux motors. Section V concludes the paper with conclusions and discussions derived from the findings.

II. Rotational Magnetic Property Measurement System

To assess the magnetic properties of material samples under 2D rotating magnetic fields, researchers have devised several rotational magnetic property measurement systems [21-23]. Among these methods, the measurement of magnetic field quantities, specifically the x-axis and y-axis components encompassing magnetic flux density (Bx, By) and field strength (Hx, Hy), has emerged as a particularly convenient approach. Illustrated in Fig. 1 is the 2D rotational magnetic property measurement system developed at the University of Technology Sydney (UTS) [22]. This system enables the generation of circular or elliptical rotational flux density vectors of different magnitudes and frequencies by controlling the magnitudes and phase angles of excitation currents within the X-axis and Y-axis coils.

In certain motor designs known as 3D magnetic flux motors, such as claw pole and transverse flux motors, the magnetic field extends throughout the three-dimensional space, with significant components along all three coordinate axes [24]. Illustrated in Fig. 2 is a cross-sectional view depicting the structure of a 3D magnetic property testing system developed at UTS [25]. This system enables the manipulation of currents within three excitation coils wound around the x-axis yoke, y-axis yoke, and z-axis yoke, respectively. Through control of the magnitudes and phase angles of these currents, the system is capable of generating spherically or ellipsoidally shaped 3D flux density loci at varying magnitudes and frequencies.

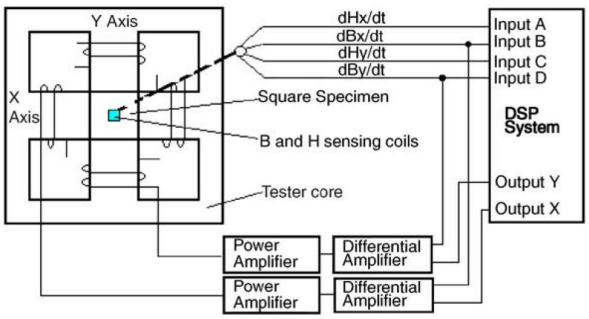

Fig. 1. Schematic diagram of a 2D rotating magnetic property measurement system.

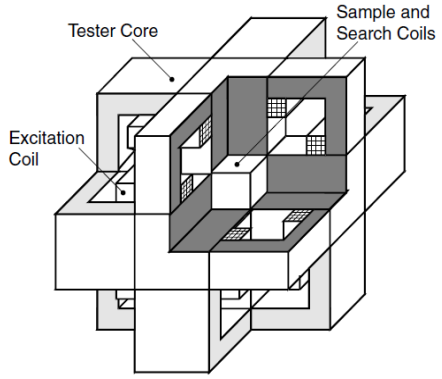

Fig. 2. Structure of a 3D rotational magnetic property testing system.

III. Vectorial Magnetic Properties

By employing the aforementioned testing systems, the 2D/3D vectorial magnetic properties of several electromagnetic materials have been investigated. In Fig. 3, the core losses of a squared single sheet sample of soft magnetic composite (SMC) material are depicted in relation to various magnitudes and frequencies of magnetic flux density (B). Fig. 3(a) illustrates the core losses under 1D alternating sinusoidal B, while Fig. 3(b) represents the losses under 2D circularly rotational B [26]. It is seen that the core loss patterns exhibit notable distinctions between 1D alternating magnetization and 2D rotating magnetization. In the low to middle range of B, the rotational core loss is approximately twice that of its alternating counterpart of the same B magnitude and frequency. However, at higher B, specifically when the material saturates, the rotational core loss diminishes rapidly, whereas the alternating counterpart continues to increase with the rise of B.

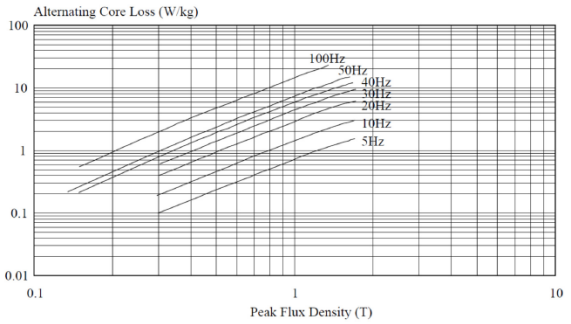

(a)

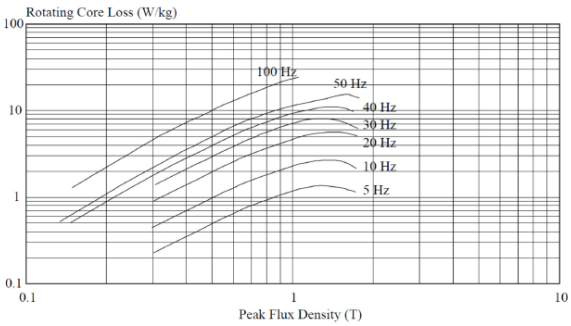

(b)

Fig. 3 Measured core losses of an SMC material sample with (a) 1D alternating B, (b) 2D circularly rotating B.

In the context of designing and analyzing rotational electrical machines, a formulation for rotational hysteresis loss has been introduced to characterize the rotational core losses. This formulation is inspired by the torque/slip curve of a single-phase induction motor [12].

Fig. 4 depicts the measured core losses of a sample of Fe-based amorphous ferromagnetic material, and analogous findings have been consistently replicated. Specifically, the rotational core losses exhibit distinct behavior from their alternating counterparts [27]. In response to this observation, a novel mathematical model has been introduced, which is grounded in the resemblance between the curves of the hysteresis core loss and the mechanical power of a three-phase induction motor.

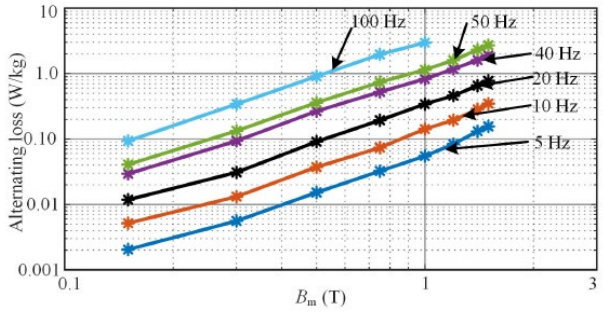

Fig. 4. Measured core losses of an Fe-based amorphous ferromagnetic material sample under (a) 1D alternating sinusoidal B; (b) 2D circularly rotational B.

Given that the magnetic field in an electrical machine inherently exists in three dimensions, comprehending the 3D vectorial magnetic properties holds both theoretical and practical significance to fully harness the potentials of electromagnetic materials. Through the utilization of the developed 3D tester in Fig. 2, it becomes possible to acquire quasi-3D and 3D properties of a cubic SMC sample, along with the 2D vectorial properties and 1D alternating properties as their specific cases [28-30].

Fig. 5 presents several measurement results, encompassing (a) the B-H curves along the x-axis, y-axis, or z-axis when the magnetic flux density (B) is sinusoidally and alternately controlled along one of the coordinate axes, (b) the corresponding B and H loci in the xoy, yoz, or zox plane when B is circularly rotationally controlled in one of the coordinate planes, and (c) the corresponding B and H loci when B is controlled to form a sphere in the 3D space.

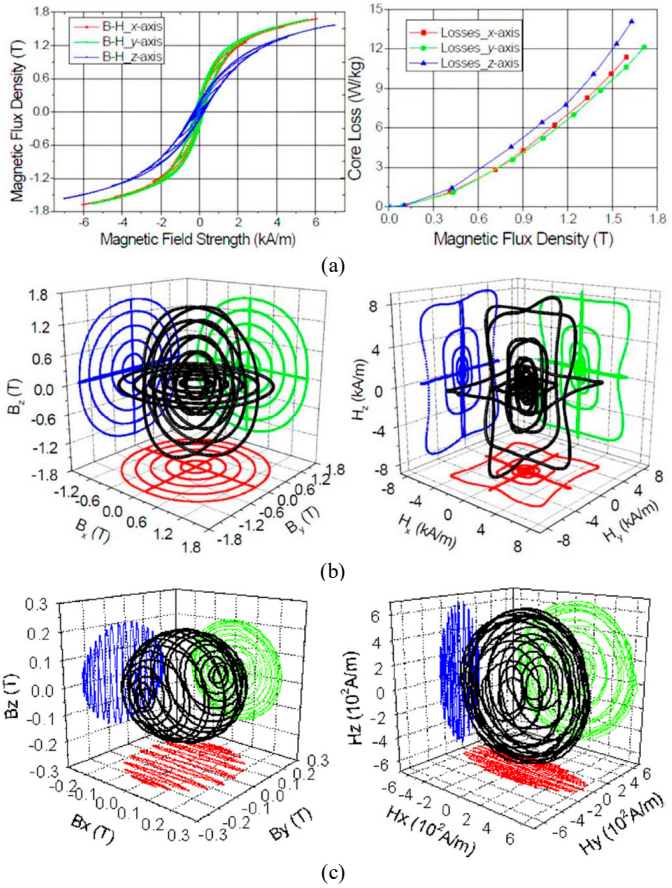

Fig. 5. Measured magnetic properties of a cubic SMC sample using the UTS 3D magnetic tester, (a) B-H relation and associated power loss with 1D alternating B, (b) Corresponding B and H loci with 2D circularly rotating B, and (c) Corresponding B and H loci in 3D space with spherical B.

IV. Vectorial Magnetic Property Modeling and Application in Design of 3D Flux Electric Motors

A. Core Loss Modeling Considering Rotating Fluxes

The core loss is typically divided into three components: hysteresis loss, eddy current loss, and anomalous loss. The primary distinction between rotational and alternating losses often lies in the hysteresis loss [12]. Below is a mathematical model for calculating the rotational core loss, P_{hr}, where f is the excitation frequency, B_s is the saturation flux density, and a_1, a_2 , and a_3 are coefficients determined by fitting data obtained from the 2D testing system shown in Fig. 1.

$$\frac{P_{hr}}{f} = a_1 \left[\frac{\frac{1}{s}}{\left(a_2 + \frac{1}{s}\right)^2 + a_3^2} - \frac{\frac{1}{(2-s)}}{\left[a_2 + \frac{1}{(2-s)}\right]^2 + a_3^2} \right] \tag{1}$$

$$s = 1 - \frac{B_P}{B_s}\sqrt{1 - \frac{1}{a_2^2 + a_3^2}} \tag{2}$$

To analyze the core losses in a rotating motor, the magnetic properties of the core materials under both 1D alternating and 2D circularly rotating flux densities should be considered, as

shown in Fig. 3. The following formulae demonstrate the calculation of core losses in an electric motor with 2D/3D rotational magnetic fields. First, 3D finite element magnetic field analysis (FEA) is conducted to calculate the flux density in each element within the core region over one electrical period. This involves repeating the FEA multiple times as the rotor is shifted by 360 electrical degrees. It is observed that the flux density vector in an element traces an irregular 3D locus, which can be projected onto three coordinate axes. Since each of the three flux density components is a periodic function, Fourier Series analysis can be employed to determine the harmonics as follows:

$$\begin{cases} B_r(t) = \sum_{k=0}^{\infty}\left[B_{rsk}\sin(2\pi k f_s t) + B_{rck}\cos(2\pi k f_s t)\right] \\ B_\theta(t) = \sum_{k=0}^{\infty}\left[B_{\theta sk}\sin(2\pi k f_s t) + B_{\theta ck}\cos(2\pi k f_s t)\right] \\ B_z(t) = \sum_{k=0}^{\infty}\left[B_{zsk}\sin(2\pi k f_s t) + B_{zck}\cos(2\pi k f_s t)\right] \end{cases} \quad (3)$$

In (3), k represents the harmonic order and f_s is the frequency of the fundamental component of the flux density. For each harmonic, the three components can be divided into two parts that are perpendicular to each other:

$$\begin{cases} B_{sk} = \boldsymbol{n_{sk}}\sqrt{B_{rsk}^2 + B_{\theta sk}^2 + B_{zsk}^2}\sin(2\pi k f_s t) \\ B_{ck} = \boldsymbol{n_{ck}}\sqrt{B_{rck}^2 + B_{\theta ck}^2 + B_{zck}^2}\cos(2\pi k f_s t) \end{cases} \quad (4)$$

These two parts form an ellipse, with the larger of $|B_{sk}|$ and $|B_{ck}|$ as the major axis B_{kmaj} and the other as the minor axis B_{kmin}. The core loss under the k-th order elliptically rotating field can be predicted by

$$P_k = P_{rk}R_{BK} + (1 - R_{BK})^2 P_{ak} \quad (5)$$

In (5), R_{BK}=B_{kmin}/B_{kmaj} represents the axis ratio, P_{rk} is the core loss under a circularly rotating flux density with magnitude B_P=B_{kmaj} and frequency f=kf_s, which can be calculated using (6), (1) and (2), and P_{ak} is the core loss under an alternating flux density with B_{kmaj} and kfs, which can be calculated using (7).

$$P_r = P_{hr} + C_{er}\left(fB_P\right)^2 + C_{ar}\left(fB_P\right)^{1.5} \quad (6)$$

$$P_a = C_{ha} f B_P^h + C_{ea}\left(fB_P\right)^2 + C_{aa}\left(fB_P\right)^{1.5} \quad (7)$$

All the coefficients C_{er}, C_{ar}, C_{ha}, h, C_{ea} and C_{aa} can be obtained by curve-fitting data as measured in the material sample. Once the core loss caused by each harmonic is worked out, the total core loss by the 3D irregular loop can be obtained by summing the core losses caused by the fundament and all harmonic components. The total core loss in the motor core is then calculated by

$$P_t = \sum_{e=1}^{Ne}\sum_{k=0}^{\infty}\left[P_{rk}R_{BK} + (1 - R_{BK})^2 P_{ak}\right] \quad (8)$$

where N_e is the number of elements in the motor core.

B. *Core Losses of Electric Motors with 3D Magnetic Flux*

The models presented above have been effectively utilized to calculate 3D magnetic flux in electric motors with high accuracy, closely aligning with experimental results from motor prototypes, such as a permanent magnet claw pole motor with an SMC stator [31]. Soft magnetic composites (SMCs) exhibit several distinctive advantages, including 3D magnetic and thermal isotropies due to their powdered composition, minimal eddy current losses, and relatively low total core losses at medium to high frequencies, thanks to the insulation coating on each particle. Additionally, SMCs offer the potential for cost-effective mass production through molding and 3D printing techniques, making them highly suitable for developing electric motors with 3D magnetic fluxes [32].

Fig. 6(a) illustrates the magnetic field finite element analysis region of one pole pitch of the motor for calculating the B locus in each element when the rotor rotates by 360 electrical degrees. As an example, Fig. 6(b) plots the calculated B locus at point C located in the claw pole part as marked in Fig. 6(a), which is a locus in 3D space.

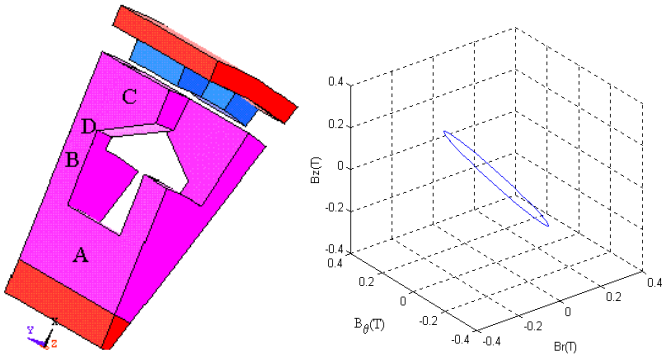

(a) (b)

Fig. 6. Analysis of a permanent magnet claw pole motor, (a) magnetic field FEA region of one pole pitch, and (b) calculated flux density locus at Point C located in the claw pole part.

Using models (1) through (8), the core loss of the SMC claw pole motor has been computed at various speeds and loads. For instance, at the rated speed of 1800 rev/min, the no-load core loss is calculated to be 59.2 W, which closely matches the measured value of 61.0 W [31]. Core losses at other speeds also align well with experimental data. Additionally, core losses under different load conditions can be computed in a similar manner, after the magnetic flux density patterns under load conditions have been analyzed using finite element analysis.

Another example involves the core loss analysis of a permanent magnet transverse flux motor with an SMC core [33,34]. Fig. 7(a) shows a region of one pole pair for 3D magnetic field finite element analysis, while Fig. 7(b) depicts the flux density trajectory at point B, as indicated in Fig. 7(a), over one full period of 360 electrical degrees. The results reveal that the magnetic flux density patterns are basically rotational and form a closed loop in 3D space.

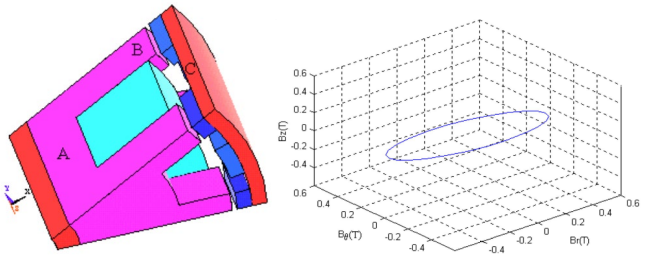

(a) (b)

Fig. 7. Analysis of a permanent magnet transverse flux motor, (a) magnetic field FEA region of one pole-pair, and (b) calculated flux density locus at Point B located in the stator tooth.

C. Magnetic Reluctivity with 3D Magnetization

Magnetic reluctivity, or permeability, typically describes the relationship between magnetic flux density (B) and magnetic field strength (H). However, since the rotational vectors of B and H are usually not aligned and their paths often form irregular loops in 3D space, the B-H relationship should be expressed using a tensor [35-37], as outlined below:

$$H_i = \sum_j v_{ij} B_j \tag{9}$$

where v_{ij} (with i=x,y,z in Cartesian coordinates, or r,θ,z in cylindrical coordinates) denotes the reluctivity tensor, which is a 3×3 matrix. In the context of static magnetic field analysis and based on Maxwell's equations, the relationship between the magnetic vector potential **A** and the applied current density vector $\mathbf{J_0}$ can be derived as follows

$$\nabla \times (v \nabla \times A) = \boldsymbol{J_0} \tag{10}$$

In rectangular coordinates, the equation for the x-component of $\mathbf{J_0}$ is given by (11). Similarly, the equations for the y- and z-components of $\mathbf{J_0}$ can be derived in the same manner.

$$\begin{aligned} &\frac{\partial}{\partial y}\left[v_{zx}\left(\frac{\partial A_z}{\partial y}-\frac{\partial A_y}{\partial z}\right)+v_{zy}\left(\frac{\partial A_x}{\partial z}-\frac{\partial A_z}{\partial x}\right)+v_{zz}\left(\frac{\partial A_y}{\partial x}-\frac{\partial A_x}{\partial y}\right)\right] \\ &-\frac{\partial}{\partial z}\left[v_{yx}\left(\frac{\partial A_z}{\partial y}-\frac{\partial A_y}{\partial z}\right)+v_{yy}\left(\frac{\partial A_x}{\partial z}-\frac{\partial A_z}{\partial x}\right)+v_{yz}\left(\frac{\partial A_y}{\partial x}-\frac{\partial A_x}{\partial y}\right)\right]=J_x \end{aligned} \tag{11}$$

V. Discussion and Conclusion

The accurate models of these materials are critical for the design optimization of various motors, such as permanent magnet motors with SMC cores [38-40]. Based on our previous work, we found that the performance of SMC motors can be improved significantly through multidisciplinary optimization [41,42]. Meanwhile, the material performance of the SMC cores depends on the manufacturing conditions, which results in material diversities that can affect the motor performance under batch production. To improve the manufacturing quality of SMC motors with high performance, robust design optimization methods, like the Taguchi method and design for six-sigma, have been investigated in our previous work [43-48].

This paper underscores the significance of comprehending the 2D/3D vectorial properties of electromagnetic materials in the context of advancing high-performance electric motors for EVs. It delves into research efforts focused on both experimental measurements and mathematical modeling of these vectorial magnetic properties. In the realm of electrical machines, where magnetic fields exhibit a 2D/3D and rotational nature, gaining insight into the behavior of electromagnetic materials during actual magnetization becomes imperative.

Contrary to the commonly employed 1D properties, the investigation reveals substantial disparities in the 2D/3D vectorial magnetic properties. Recognizing these distinctions becomes pivotal in achieving a comprehensive understanding of electromagnetic material responses under real-world magnetization conditions. This exploration carries not only theoretical significance but also practical implications, offering valuable insights for the advanced design, analysis, and optimization of high-performance electrical machines.

References

[1] D. Tan, "Transportation electrification: challenges and opportunities," *IEEE Power Electron. Mag.*, vol. 3, pp. 50-52, 2016.

[2] B. Bilgin and A. Emadi, "Electric motors in electrified transportation: a step toward achieving a sustainable and highly efficient transportation system," *IEEE Power Electron. Mag.*, vol. 1, pp. 10-20, 2014.

[3] A.T. Wilder, "Materials for advanced electric machines: an overview," in *Proc. 2005 IEEE Electric Ship Transportation Symposium (ESTS)*, Philadelphia, USA, 27 Jul. 2005, pp. 478-480.

[4] A.M. EL-Refaie, "Role of advanced materials in electrical machines," in *Proc. 20th Int. Conf. Electrical Machines and Systems (ICEMS)*, Sydney, Australia, 11-14 Aug. 2017, pp. 1-6.

[5] H. Zhao, C. Chu, H.H. Eldeeb, Y. Zhan, G. Xu, and O.A. Mohammed, "Optimal design of high-speed solid-rotor cage induction motors considering ferromagnetic materials behavior and manufacturing process," *IEEE Trans. Ind. Applicat.*, vol. 56, no. 4, pp. 4345-4355, 2020.

[6] M. Enokizono, D. Wakabayashi, N. Soda, Y. Tsuchida, S. Ueno, and M. Oka, "High power density and high efficiency of high speed motor," in *Proc. Int. Conf. Electrical Machines*, 23-26 Aug. 2020, pp. 170-176.

[7] Y. Guo, L, Liu, X. Ba, H. Lu, G. Lei, W. Yin, and J. Zhu, "Design high-power-density electric motors for electric vehicles with advanced magnetic materials," *World Electric Vehicle Journal*, vol. 14, article 114, 2023.

[8] Y. Guo, L, Liu, W. Yin, H. Lu, G. Lei, and J. Zhu, "Designing high-power-density electromagnetic devicess with nnaocrystalline and amorphous magnetic materials," *Nanomaterials*, vol. 13, article 1963, 2023.

[9] ASTM A343-97, "Standard test method for alternating-current magnetic properties of material at power frequencies using wattmeter-ammeter-voltmeter method and 25-cm Epstein test frame," American Society for Testing and Materials, West Conshohocken, PA, USA, 2000.

[10] T.L. Mthombeni, P. Pillay, and R.M.W. Strnat, "New Epstein frame for lamination core loss measurements under high frequencies and high flux densities," *IEEE Trans. Energy Convers.*, vol. 22, no. 3, pp. 614-620, 2007.

[11] G. Bertotti, A. Boglietti, M. Chiampi, D. Chiarabaglio, F. Fiorillo, and M. Lazzari, "An improved estimation of iron losses in rotating electrical machines," *IEEE Trans. Magn.*, vol. 27, no. 6, pp. 5007-5009, Nov. 1991.

[12] J.G. Zhu and V.S. Ramsden, "Improved formulations for rotational core losses in rotating electrical machines," *IEEE Trans. Magn.*, vol. 34, no. 4, pp. 2234-2242, Jul. 1998.

[13] Y.G. Guo, J.G. Zhu, Z.W. Lin, and J.J. Zhong, "Measurement and modeling of core losses of soft magnetic composites under 3-D magnetic

excitations in rotating motors," *IEEE Trans. Magn.*, vol. 41, no. 10, pp. 3925-3927, Oct. 2005.

[14] Y. Li, J. Zhu, Q. Yang, Z. Lin, Y. Guo, and Y. Wang, "Measurement of soft magnetic composite material using an improved 3D tester with flexible excitation coils and novel sensing coils," *IEEE Trans. Magn.*, vol. 46, no. 6, pp. 1971-1974, Jun. 2010.

[15] Y. Guo, L. Liu, X. Ba, H. Lu, G. Lei, W. Yin, and J. Zhu, "Measurement and modeling of magnetic materials under 3D vectorial magnetization for electrical machine design and analysis," *Energies*, vol. 16, article 417, 2023.

[16] S. Ueno, M. Enokizono, Y. Mori, and K. Yamazaki, "Vector magnetic characteristics of ultra-thin electrical steel sheet for development of high-efficiency high-speed motor," *IEEE Trans. Magn.*, vol. 53, no. 11, article 6300604, Nov. 2017.

[17] B. Eberleh and T. Hartkopf, "A high speed induction machine with two speed transmission as drive for electric vehicles," in *Proc. Int. Symp. Power Electronics, Electrical Drives, Automation and Motion*, Taormina, Italy, 23-26 May 2006, pp. 249-254.

[18] Y. Huang, J. Zhu, and Y. Guo, "Thermal analysis of high-speed SMC motor based on thermal network and 3-D FEA with rotational core loss included," *IEEE Trans. Magn.*, vol. 45, no. 10, pp. 4680-4683, Oct. 2009.

[19] M. Enokizono, "Necessary condition for development of high efficiency, high density and high speed motor," in *Proc. IEEE Int. Workshop Electrical Machines Design, Control and Diagnosis (WEMDCD)*, Athens, Greece, 22-23 Apr. 2019, pp. 60-64.

[20] Y. Guo, J. Zhu, G. Lei, H. Lu, and J. Jin, "Characterization of electromagnetic materials under 2D/3D rotational magnetization," in *Proc. IEEE Int. Conf. Applied Superconductivity and electromagnetic devices*, Tianjin, China, 27-29 Oct. 2023, pp. 1-2.

[21] M. Enokizono, T. Suzuki, J. Sievert, and J. Xu, "Rotational power loss of silicon steel sheet," *IEEE Trans. Magn.*, vol. 26, no. 5, pp. 2562-2564, Sep. 1990.

[22] J.G. Zhu, J.J. Zhong, V.S. Ramsden, Y.G. Guo, "Power losses of soft magnetic composite materials under two-dimensional excitation," *J. Applied Physics*, vo. 85, no. 8, pp. 4403-4405, Apr. 1999.

[23] D. Zhang, K. Shi, Z. Ren, M. Jia, C.-S. Koh, and Y. Zhang, "Measurement of stress and temperature dependent vector magnetic properties of electrical steel sheet," *IEEE Trans. Ind. Electronics*, vol. 69, no. 1, pp. 980-990, Jan. 2022.

[24] Y.G. Guo, J.G. Zhu, P.A. Wattersom, and W. Wu, "Comparative study of 3-D flux electrical machines with soft magnetic composite core," *IEEE Trans. Ind. Applicat.*, vol. 39, no. 6, pp. 1696-1703, Nov. 2003.

[25] J.G. Zhu, J.J. Zhong, Z.W. Lin, and J.D. Sievert, "Measurement of magnetic properties under 3-D magnetic excitations," *IEEE Trans. Magn.*, vol. 39, no. 5, pp. 3429-3431, Sep. 2003.

[26] Y. Guo, J. Zhu, H. Lu, Z. Lin, and Y. Li, "Core loss calculation for soft magnetic composite electrical machines," *IEEE Trans. Magn.*, vol. 48, no. 11, pp. 3112-3115, Nov. 2012.

[27] P.C. Sarker, Y. Guo, H.Y. Lu, and J.G. Zhu, "Measurement and modeling of rotational core loss of Fe-based amorphous magnetic material under 2-D magnetic excitation," *IEEE Trans. Magn.*, vol. 57, no. 11, article 8402008, Nov. 2012.

[28] Y. G. Guo, J. G. Zhu, Z. W. Lin, and J. J. Zhong, "3D vector magnetic properties of soft magnetic composite material," *J. Magnetism and Magnetic Materials*, vol. 302, pp. 511-516, 2006.

[29] Y. Li, J. Zhu, Q. Yang, Z. W. Lin, Y. Guo, and C. Zhang, "Study on rotational hysteresis and core loss under three-dimensional magnetization," *IEEE Trans. Magn.*, vol. 47, no. 10, pp. 3520-3523, Oct. 2011.

[30] Y. Li, Q. Yang, J. Zhu, and Y. Guo, "Magnetic properties measurement of soft magnetic materials over wide range of excitation frequency," *IEEE Trans. Ind. Applicant.*, vol. 48, no. 1, pp. 88-97, Jan. 2012.

[31] Y. G. Guo, J. G. Zhu, P. A. Watterson, and W. Wu, "Development of a permanent magnet claw pole with soft magnetic composite core," *Australian J. Electrical & Electronic Eng.*, vol. 2, no. 1, pp. 21-30, 2005.

[32] Y. Guo, X. Ba, L, Liu, H. Lu, G. Lei, W. Yin, and J. Zhu, "A review of electric motors with soft magnetic composite cores for electric drives," *Energies*, vol. 16, article 2053, 2023.

[33] J.G. Zhu, Y.G. Guo, Z.W. Lin, Y.J. Li, and Y.K. Huang, "Development of PM transverse flux motors with soft magnetic composite cores," *IEEE Trans. Magn.*, vol. 47, no. 10, pp. 3248-3251, Oct. 2011.

[34] Y.G. Guo, J.G. Zhu, H.Y. Lu, Y.J. Li, and J.X. Jin, "Core loss computation in a permanent magnet transveres flux motor with rotating fluxes," *IEEE Trans. Magn.*, vol. 50, no. 11, article 6971480, Nov. 2014.

[35] M. Enokizono and S. Mori, "A treatment of the magnetic reluctivity tensor for rotating magnetic field," *IEEE Trans. Magn.*, vol. 33, pp. 1608-1611, 1997.

[36] Y. Guo, J.G. Zhu, Z.W. Lin, J.J. Zhong, H.Y. Lu, and S. Wang, "Determination of 3D magnetic reluctivity tensor of soft magnetic composite material," *J. Magn. Magm. Mater.*, vol. 312, pp. 458-463, 2007.

[37] J.B. Padilha, P. Kuo-Peng, N. Sadowski, and N.J. Batistela, "Vector hysteresis model assocaited to FEM in a hysteresis motor modeling," *IEEE Trans. Magn.*, vol. 53, article 7402004, 2017.

[38] G. Lei, C. Liu, J. Zhu, and Y. Guo, "Techniques for multilevel design optimization of permanent magnet motors," *IEEE Trans. Energy Convers.*, vol. 30, no. 4, pp. 1574-1584, Dec. 2015.

[39] G. Lei, T. Wang, J. Zhu, Y. Guo, and S. Wang, "System-level design optimization method for electrical drive systems—robust approach," *IEEE Trans. Ind. Electronics*, vol. 62, no. 8, pp. 4702-4713, Aug. 2015.

[40] G. Lei, T. Wang, Y. Guo, J. Zhu, and S. Wang, "System-level design optimization methods for electrical drive systems: deterministic approach," *IEEE Trans. Ind. Electronics*, vol. 61, no. 12, pp. 6591-6602, Dec. 2014.

[41] G. Lei, C. Liu, Y. Guo, and J. Zhu, "Multidisciplinary design analysis and optimization of a PM transverse flux machine with soft magnetic composite core," *IEEE Trans. Magn.*, vol. 51, no. 11, pp. 1-4, Nov. 2015.

[42] G. Lei, C. Liu, Y. Guo, and J. Zhu, "Robust multidisciplinary design optimization of PM machines with soft magnetic composite cores for batch production," *IEEE Trans. Magn.*, vol. 52, no. 3, pp. 1-4, Mar. 2016, Art no. 8101304.

[43] B. Ma, G. Lei, J. Zhu, Y. Guo, and C. Liu, "Application-oriented robust design optimization method for batch production of permanent-magnet motors," *IEEE Trans. Ind. Electronics*, vol. 65, no. 2, pp. 1728-1739, Feb. 2018.

[44] B. Ma, G. Lei, C. Liu, J. Zhu, and Y. Guo, "Robust tolerance design optimization of a PM claw pole motor with soft magnetic composite cores," *IEEE Trans. Magn.*, vol. 54, no. 3, pp. 1-4, Mar. 2018, Art no. 8102404.

[45] G. Lei, J. Zhu, Y. Guo, K. Shao, and W. Xu, "Multiobjective sequential design optimization of PM-SMC motors for six Sigma quality manufacturing," *IEEE Trans. Magn.*, vol. 50, no. 2, pp. 717-720, Feb. 2014.

[46] G. Lei, J. G. Zhu, Y. G. Guo, J. F. Hu, W. Xu, and K. R. Shao, "Robust design optimization of PM-SMC motors for six Sigma auality manufacturing," *IEEE Trans. Magn.*, vol. 49, no. 7, pp. 3953-3956, July 2013.

[47] G. Lei, G. Bramerdorfer, B. Ma, Y. Guo, and J. Zhu, "Robust design optimization of electrical machines: multi-objective approach," *IEEE Trans. Energy Convers.*, vol. 36, no. 1, pp. 390-401, Mar. 2021.

[48] G. Lei, G. Bramerdorfer, C. Liu, Y. Guo, and J. Zhu, "Robust design optimization of electrical machines: a comparative study and space reduction strategy," *IEEE Trans. Energy Convers.*, vol. 36, no. 1, pp. 300-313, Mar. 2021.